



Experimental and modeling study on ignition delays of lean mixtures of methane, hydrogen, oxygen, and argon at elevated pressures

Yingjia Zhang^a, Zuohua Huang^{a,*}, Liangjie Wei^a, Jiaxiang Zhang^a, Chung K. Law^b

^a State Key Laboratory of Multiphase Flow in Power Engineering, Xi'an Jiaotong University, Xi'an 710049, People's Republic of China

^b Dept. of Mechanical and Aerospace Engineering, Princeton University, Princeton, NJ 08540-5263, United States

ARTICLE INFO

Article history:

Received 17 June 2011

Received in revised form 30 July 2011

Accepted 17 September 2011

Available online 8 October 2011

Keywords:

Ignition delay

Methane

Hydrogen

Shock tube

Chemical kinetics

ABSTRACT

Ignition delays of lean mixtures of methane–hydrogen with various hydrogen volumetric contents were experimentally studied in a shock tube together with modeling analysis. Results show that the ignition behavior of the methane–hydrogen mixture depending on pressure resembles that of methane for hydrogen fraction less than 40%, with the ignition delays decreasing with increasing pressure. For the hydrogen fraction equal 60%, a negligible promoted effect of pressure on the ignition of the methane–hydrogen mixture is exhibited. For hydrogen fractions equal or greater than 80%, however, the ignition response resembles that of hydrogen in that the ignition delay exhibits a complex dependence on pressure and two-step transition in the global activation energy. Compared with calculated values using four available mechanisms, the NUI Galway mechanism yielded the closest agreement, and was adopted in the sensitivity analysis of the ignition kinetics. The sensitivity analysis well explained the experimental results which the ignition delay decreases with increasing temperature regardless of whether methane (typical fuel 80%CH₄/20%H₂) or hydrogen (typical fuel 20%CH₄/80%H₂) dominates the ignition process. Rate of production analysis shows that the promoted effect of the hydrogen on the oxidation of the methane is mainly due to the concentrations of the free radicals such as H, O and OH increase with increasing hydrogen fraction, and lead to the total reaction rate is enhanced. Consumption of methane is mainly through these reactions in which the active free radicals participate.

© 2011 The Combustion Institute. Published by Elsevier Inc. All rights reserved.

0. Introduction

Natural gas has been widely used in the automobile engines due to its high octane number, high anti-knock capability and low pollutant emissions [1–4]. However, it also has some unfavorable combustion characteristics, such as low auto-ignition temperature and low flame propagation speed at lean mixture and poor lean burn capability, due to its high C–H bond energy. These could lead to an increased cycle-to-cycle variations, reduced thermal efficiency, reduced power output and increased HC emission under lean-mixture combustion in spark ignition engines. Hydrogen, which has the fastest flame speed among practical fuels, can be mixed in natural gas and/or methane to increase the overall flame speed, extend the lean burn limit and increase the fraction of exhaust gas recirculation. This approach has been reported in spark ignition engines and homogeneous charge ignition engines [5–12]. It is well known that the tendency to knock increases with the hydrogen addition. The knocking combustion in spark ignited engine is closely related to auto-ignition of the unburned gas. Therefore, the auto-ignition delay of the methane–hydrogen mixtures

should be clearly understood. Furthermore, Utilization of methane–hydrogen mixture can also serve as a transitional measure before pure hydrogen is utilized in engines.

A number of fundamental combustion studies of methane–hydrogen mixtures have been conducted on laminar burning velocities [13–18], radical concentrations [19,20] and simulation [21–24]. However, there have been few experimental investigations on the ignition characteristics and chemistry for methane–hydrogen mixtures. Fotache et al. [25] experimentally studied the ignition of hydrogen addition to methane in nonpremixed, counterflow jets at pressures from 0.02 to 0.8 MPa with pressure-weighted strain rates from 150 to 350 s⁻¹ and hydrogen fraction from 0% to 60% in volume. Three ignition regimes depending on the hydrogen fraction were found. Gersen et al. [26] measured the ignition delay of methane/hydrogen mixtures in a rapid compression machine under stoichiometric conditions at pressures from 1.5 to 7.0 MPa, temperatures from 950 to 1060 K, and hydrogen mole fractions from 0% to 100%. Their results showed that the promoted effect of hydrogen is only marginal for hydrogen fraction below 20%, while the ignition delay decreased remarkably when the hydrogen fraction is over 50%. Furthermore, the facilitated ignition is enhanced with increasing temperature and is reduced with increasing pressure. Lifshitz et al. [27] investigated

* Corresponding author. Fax: +86 29 82668789.

E-mail address: zhhuang@mail.xjtu.edu.cn (Z. Huang).

the high-temperature ignition characteristics of methane/hydrogen/oxygen mixtures using a shock tube. The conditions behind the reflected shock waves cover the temperature range from 1597 to 1805 K under the pressure of 185 Torr. The effect of hydrogen addition on ignition was interpreted based on thermal consideration. Cheng and Oppenheim [28] experimentally measured the ignition delays and found a strong ignition limit of methane/hydrogen/oxygen mixtures in shock tube at pressures from 0.1 to 0.3 MPa and temperatures from 800 to 2400 K. They proposed the following Arrhenius-type correlation based on methane/oxygen and hydrogen/oxygen:

$$\tau = \tau_{\text{CH}_4}^{(1-\zeta)} \tau_{\text{H}_2}^{\zeta}$$

where ζ is the mole fraction of hydrogen in the fuel blend, and τ_{CH_4} and τ_{H_2} are the ignition delays of methane and hydrogen respectively. Huang et al. [29] conducted both experimental and numerical studies for two stoichiometric methane–hydrogen mixtures in a shock tube at pressures from 1.6 to 4.0 MPa and temperatures from 1000 to 1300 K, and hydrogen mole fractions from 15% to 35%. Their results showed that a promoted effect of hydrogen addition on the reduction of ignition delays, and the reduction rate is decreased with decreasing temperature at 35% hydrogen fraction. Chaumeix et al. [30] measured the ignition delays and investigated the detonation properties of methane/hydrogen/oxygen mixtures, using argon as the diluted gas. The experimental conditions cover the temperatures from 1250 to 2000 K and pressures from 0.15 to 1.6 MPa behind the reflected shock waves. The detonation speed and cell size were determined, and the ignition delays were compared to the predicted values from four models. It was found that the Konnov's model agrees well with the experimental data. They suggested that methane might significantly inhibit the detonation processes of the combustible mixtures. Petersen et al. [31] experimentally measured the ignition delays of methane/hydrogen mixtures in a shock tube. The experimental temperatures range from 1141 to 1533 K at pressure of 2.1 MPa with hydrogen fractions of 20% and 40%. Their results showed that hydrogen addition could decrease the ignition delays significantly, and the effectiveness is increased with the increasing of hydrogen fraction. They suggested that hydrogen addition did not shift the dominant kinetic regimes at the chosen experimental conditions. In other words, the global activation energy of the methane/hydrogen mixtures does not change. Herzler and Naumann [32] measured the ignition delays of methane/ethane/hydrogen mixtures with hydrogen fraction of 0%, 40%, 80% and 100% in a shock tube at temperatures range from 900 to 1800 K and pressures range from 0.1 to 1.6 MPa. They suggested that the current mechanisms could not well represent the

reduction of the global activation energy at low temperatures for the mixtures whose ignition is dominated by hydrogen kinetics.

Recognizing the limited amount of experimental and computational studies on the ignition delays of methane–hydrogen mixtures, we have performed such a study on the ignition delays for lean methane–hydrogen mixtures, with particular interest on understanding on the effects of hydrogen addition and the mechanism of hydrogen enriched combustion. Thus, in the experiment, the hydrogen fractions in the methane–hydrogen blend are 0%, 20%, 40%, 60%, 80% and 100%. The experimental conditions behind reflected shock waves cover the temperatures range from 1000 and 2000 K, and pressures range from 0.5 and 2.0 MPa. Argon is used as the diluted gas. The NUI Galway model [33] is used to simulate the ignition delays behind the reflected shock wave. Meanwhile, the sensitivity analysis, rate of production and consumption of the main radicals and concentration of the free radicals H, O and OH in the ignition process of methane–hydrogen mixtures are analyzed. Experimental and simulated results are used to explain the mechanisms of hydrogen addition and varied hydrogen fractions on the enhancement of methane ignition.

1. Experimental setup and procedures

1.1. Experimental setup

Schematic of the shock tube facility is shown in Fig. 1. The shock tube consists of a 4 m driver section separated from a 4.8 m driven section with a large diameter of 11.5 cm by a double diaphragm. Helium and nitrogen mixtures were used as the driver gases. Four fast-response piezoelectric pressure transducers, which triggered the time interval counters, were located at fixed intervals along the driven section. The chemical equilibrium software Gaseq [34] was used to calculate the temperature and pressure behind the reflected shock wave. The uncertainty of experimental temperature was calculated using a standard error analysis procedure based [35] on the uncertainty in the shock attenuation and non-ideal shock reflection from the interactions between shock wave and boundary layer [36,37]. Uncertainty of temperature behind the reflected shock waves is 25 K.

Fuel mixtures were prepared in advance in a tank according to Dalton's law of partial pressure, and the prepared mixture was allowed to settle 12 h to ensure sufficient mixing.

Ignition was monitored by the reflected shock pressure and OH* emission. The reflected shock pressure was traced by a piezoelectric pressure transducer with acceleration compensation which was located at 20 mm from the end wall of the shock tube. OH* emission

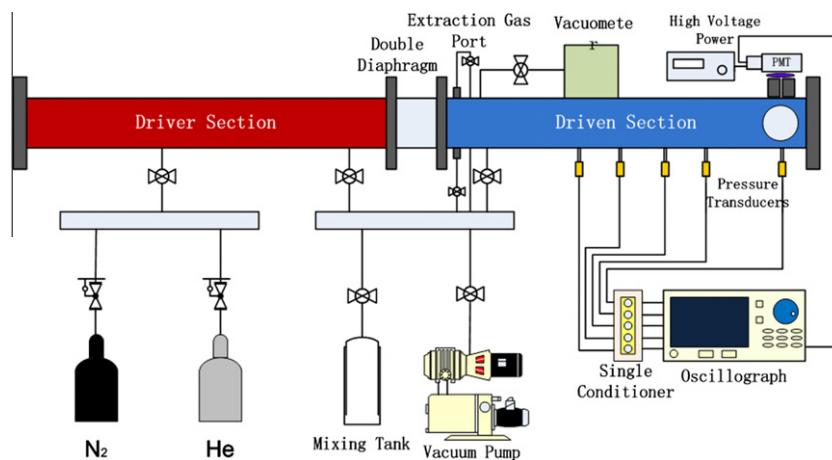


Fig. 1. Schematic of the shock tube.

with the wavelength of 307 nm was obtained with a photomultiplier through a narrow band pass filter. Previous studies showed that the emission signal is the simplest and the most reliable method to diagnose the ignition of the combustible mixture [31,38]. The tailored interface conditions were used to obtain longer effective testing time at relatively low temperature by regulating the ratio of helium and nitrogen in the driver gases [39]. This implies that only a Mach wave was generated at the contacting surface when the reflected shock wave arrives, and the conditions in the experimental region remained unchanged until the rarefaction wave arrived. The longest effective testing time was reached about 12 ms.

1.2. Ignition delay

Ignition delays of methane–hydrogen mixtures with hydrogen fractions in volume of 0%, 20%, 40%, 60%, 80% and 100% were measured. Detailed compositions of test mixtures in this study are given in Table 1. In order to obtain a reasonable and accurate ignition delay, two methods were used to derive the ignition delays at two ignition regimes. For the strong ignition mode, the ignition delay is defined as the time interval between the arrival of the reflected shock wave and the sudden rise in OH* emission, as shown in Fig. 2a. The pressure profile (black solid line) of pure hydrogen at $T = 1065$ K and $p = 1.0$ MPa shows a two-step increasing due to the incident and reflected shock waves (definition of time zero), and a constant pressure is sustained at about $1700 \mu\text{s}$. A steep rise in pressure is then observed. However, the OH* emission signal (red dash line) remains almost at zero prior to this instant and increases suddenly after ignition occurs. It is to be noted that a significant pressure rise (4%/ms) due to the facility-dependent BL (boundary layer) effect was observed from 1.5 ms behind the arrival of reflected shock wave, as seen in Fig. 2a. For the weak ignition mode, like the ignition of pure methane at $T = 1438.6$ K and $p = 1.0$ MPa in Fig. 2b, a steep increase in both pressure and OH* emission is hardly distinguished. In this case, the ignition delay is defined as the interval between arrival of the reflected shock

Table 1
Main constituents in the test mixture ($\phi = 0.5$ for all mixtures).

Mixtures	Blend	XCH ₄ (%)	XH ₂ (%)	XO ₂ (%)	XAr (%)
1	100%CH ₄	0.998	0	3.99	95.012
2	80%CH ₄ /20%H ₂	0.931	0.233	3.956	94.88
3	60%CH ₄ /40%H ₂	0.837	0.558	3.907	94.698
4	40%CH ₄ /60%H ₂	0.697	1.046	3.834	94.423
5	20%CH ₄ /80%H ₂	0.464	1.856	3.713	93.967
6	0%CH ₄	0	3.471	3.471	93.058

and the interaction timing. The interaction timing is based on the extrapolation of the maximum slope of the OH* emission signal to the zero, as shown in Fig. 2b. Both methods are reasonable and were used widely by de Vries et al. [40,41], Horning et al. [42] and Frenklach et al. [43]. Furthermore, effect of vibrational relaxation can be neglected due to the highly diluted gas (over 93% Ar in the test mixtures) [44,45].

It is noted that this definition is seemingly for the undiluted fuel-air mixtures, but the effect of gas dynamic on acceleration of ignition should be considered for the current mixtures of methane–hydrogen with highly diluted gas at high temperature [44]. The typical value of the uncertainty in ignition delay is $28 \mu\text{s}$ in the current study. Thus, the experimental data are only as reference for ignition delay less than $200 \mu\text{s}$.

2. Experimental results and analysis

2.1. Comparison with previous studies

The measured ignition delays of methane OH* are compared with the results in the literatures [27,31,46,47] to ensure the reliability of the shock tube measurement and the credibility of the data processing. Meanwhile, the experimental data are also compared with the calculated results using four available mechanisms [33,48–50], as shown in Fig. 3. Experimental temperatures are from 1369 to 2000 K at pressure of about 1.0 MPa and equivalence ratio of 0.5. Argon (mole fraction from 75% to 98%) is used as the diluted gas. Comparison shows good agreement between the current study

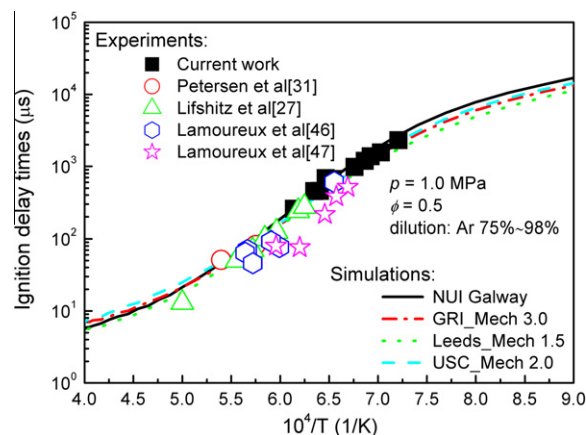


Fig. 3. Comparison on ignition delays between measured and simulated.

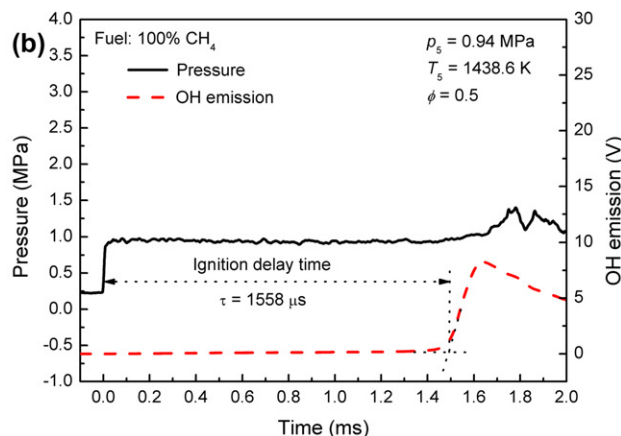
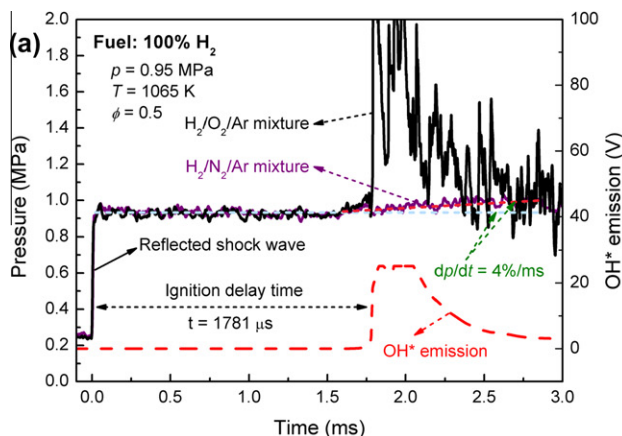


Fig. 2. Definition of ignition delays for two ignition modes. (a) Strong ignition mode, (b) weak ignition mode.

and previous experimental studies. The ignition delays obtained by Lamoureux et al. [47] yield a slightly lower value. This is due to the discrepancies in experimental conditions, methods and definition of ignition delay. For methane combustion, the four models can accurately reproduce the ignition delays.

2.2. Data analysis

Ignition delays of lean methane–hydrogen mixtures (equivalence ratio of 0.5) with hydrogen fractions from 0% to 100% were measured behind the reflected shock waves in the temperatures range of 1000–2000 K and pressures range of 0.5–2.0 MPa. Effects of pressure on the ignition delays of mixtures with various hydrogen fractions are shown in Figs. 4–9.

Figure 4 shows that the ignition delays of methane decreases significantly with increasing pressure. The ignition delays at pressures of 1.0 MPa and 2.0 MPa are less one-second and one-fourth respectively to the values at pressure of 0.5 MPa at $T = 1454$ K. This can be explained by using the Arrhenius-type correlation,

$$\tau = A \cdot p^a \phi^b X_{O_2}^c \exp \frac{E_a}{RT} \quad (1)$$

Generally, the pressure exponential a gives the negative value for the typical hydrocarbon fuel, which indicates that ignition delays decrease with the increase of pressure. The global activation energies obtained at the pressures of 0.5 MPa, 1.0 MPa and 2.0 MPa using multiple linear regression method are 48.4 kcal/mol,

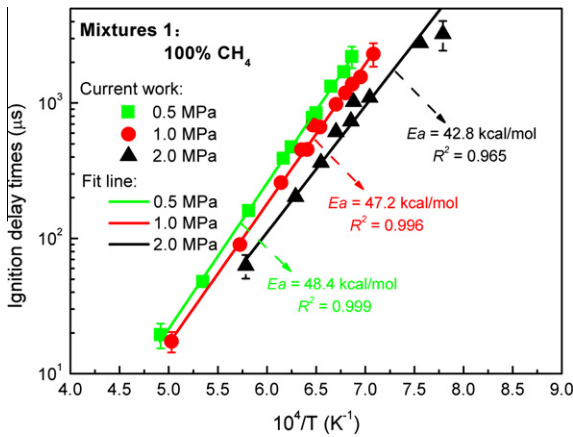


Fig. 4. Ignition delays and activation energies of methane at different pressures.

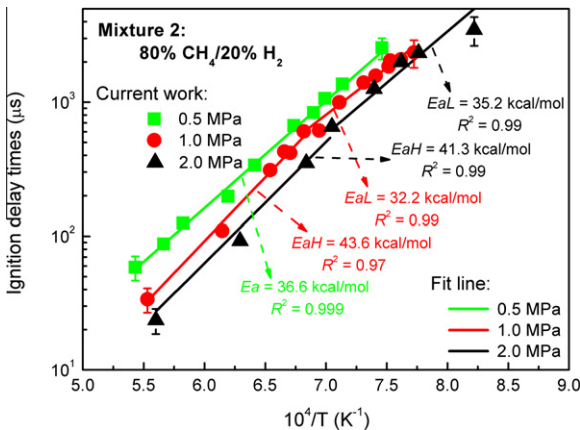


Fig. 5. Ignition delays and activation energies of 80%CH₄/20%H₂ at different pressures.

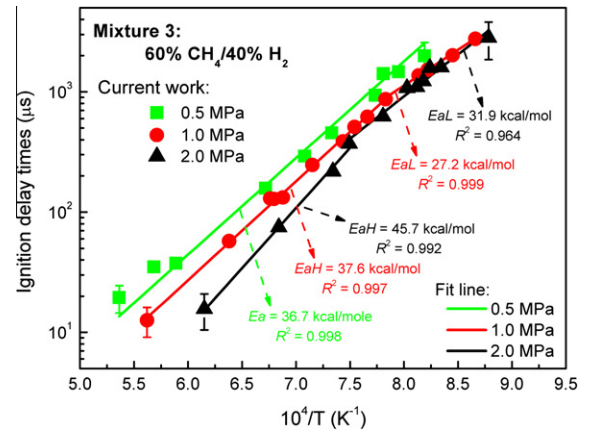


Fig. 6. Ignition delays and activation energies of 60%CH₄/40%H₂ at different pressures.

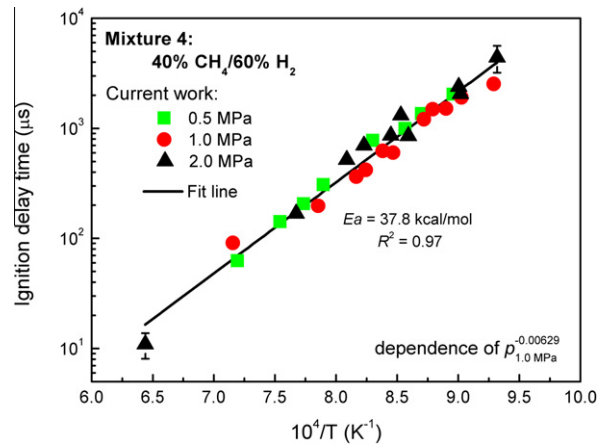


Fig. 7. Ignition delays and activation energies of 40%CH₄/60%H₂ at different pressures.

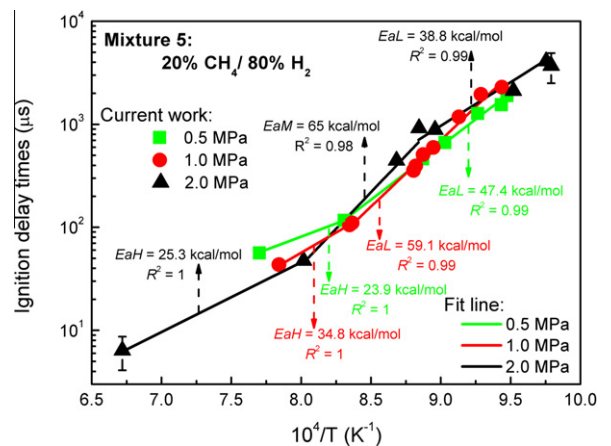


Fig. 8. Ignition delays and activation energies of 20%CH₄/80%H₂ at different pressures.

47.2 kcal/mol and 42.8 kcal/mol, respectively ($R^2 > 0.965$). The typical values of activation energy of methane are 46–54 kcal/mol in literatures [27,28,31,51–53], as shown in Table 2. Huang et al. [54] conducted an experimental study on ignition delays at relatively low temperature conditions using a shock tube, where the activation energy was less than 18 kcal/mol, and a reversed “S”

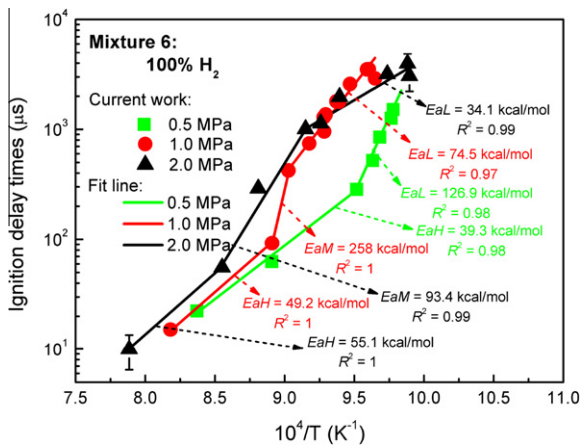


Fig. 9. Ignition delays and activation energies of hydrogen at different pressures.

Table 2
Compression of activation energy from detailed sources at wide conditions.

Source	Experimental conditions	Activation energy (kcal/mol)
Current work	$T_5 = 1290\text{--}2000\text{ K}$, $p_5 = 0.5\text{--}2.0\text{ MPa}$, $\phi = 0.5$, Ar = 80%	42.8–48.4
Grillo and Slack [51]	$T_5 = 1400\text{--}1850\text{ K}$, $p_5 = 0.4\text{ MPa}$, $\phi = 2.0$, Ar = 79–96%	53.4
Seery and Bowman [52]	$T_5 = 1350\text{--}1900\text{ K}$, $p_5 = 0.15\text{--}0.4\text{ MPa}$, $\phi = 0.2\text{--}5.0$, Ar = 53.4–78.4%	52.3
Petersen et al. [31,53]	$T_5 = 1410\text{--}2040\text{ K}$, $p_5 = 0.9\text{--}48\text{ MPa}$, $\phi = 0.5\text{--}4.0$, Ar = 89–99%, $N_2 = 97.66\%$	51.8
Lifshitz et al. [27]	$T_5 = 1500\text{--}2100\text{ K}$, $p_5 = 0.2\text{--}1.0\text{ MPa}$, $\phi = 0.5\text{--}2.0$, Ar = 89–97%	51.4
Cheng and Oppenheim [28]	$T_5 = 800\text{--}2400\text{ K}$, $p_5 = 0.1\text{--}0.3\text{ MPa}$, $\phi = 0.5\text{--}1.5$, Ar = 90%	46.4

shape characteristic for the ignition delay was presented. However, variation of the activation energy is not observed in this study, and the result of this study is consistent with that from Petersen et al. [44]. Petersen et al. suggested that the elevated temperature would not shift the kinetic regimes for the lean methane–oxygen mixtures. The difference in activation energy between this work and Huang et al. [54] is from the difference in experimental conditions. The test temperature range is from 1315 to 2000 K in this study, and the those of Huang et al. [54] is from 1000 to 1350 K. the low temperature range of this study is consistent with high temperature range of the Huang et al. [54]. It is well known that high temperature activation energy is higher than that of low temperature. The temperature range of this study is closer to that of Petersen et al. [44], which gives the consistent results between them. However, the study of Huang et al. [54] was conducted at temperature blow 1350 K, and the “S” shape characteristic is only presented at the stoichiometric equivalence ratio. It is well known that the dominant chain branching reactions are quite different in methane ignition chemistry at different temperatures. The chain branching reactions $\text{CH}_3 + \text{O}_2 \rightleftharpoons \text{O} + \text{CH}_3\text{O}$ and $\text{HO}_2 + \text{CH}_3 \rightleftharpoons \text{OH} + \text{CH}_3\text{O}$ are important when $T > 1400\text{ K}$. However, the reactions $\text{CH}_3 + \text{CH}_3\text{O}_2 \rightleftharpoons \text{CH}_3\text{O} + \text{CH}_3\text{O}$ and $\text{H}_2\text{O}_2 (+\text{M}) \rightleftharpoons \text{OH} + \text{OH} (+\text{M})$ dominate the ignition chemistry when $T < 1100\text{ K}$ [55]. Furthermore, the diluted gas and experimental setup may also affect on the results.

Similar pressure dependence of ignition delays is presented for the 20% H_2 /80% CH_4 fuel blend as shown in Fig. 5. This indicates that the methane chemistry still dominates the ignition of the 20% H_2 /

80% CH_4 fuel blend. The activation energy for the 20% H_2 /80% CH_4 fuel blend does not change at the pressure of 0.5 MPa, which gives the value of 36.6 kcal/mol. While a significant transition in activation energy is presented at $T = 1467\text{ K}$ and $T = 1419\text{ K}$ at pressures of 1.0 MPa and 2.0 MPa. At pressure of 1.0 MPa, the high temperature activation energy (EaH) of the 20% H_2 /80% CH_4 fuel blend is 43.4 kcal/mol at $T > 1467\text{ K}$, and the low temperature activation energy (EaL) is 32.2 kcal/mol at $T < 1467\text{ K}$. At pressure of 2.0 MPa, EaH takes the value of 41.3 kcal/mol at $T > 1419\text{ K}$ and EaL takes the value of 37.2 kcal/mol at $T < 1419\text{ K}$. The similar transition in activation energy was also observed by Petersen et al. [31]. They measured the ignition delays of the 20% H_2 /80% CH_4 fuel blend at pressure of 2.1 MPa. The value of EaH was 41.4 kcal/mol and the value of EaL was 31.1 kcal/mol in their study. The transition can be considered in the effect of hydrogen addition on the chain branching in the ignition process. The measured ignition delays in Petersen et al. [31] are slightly lower than those in this study, and the difference is from the difference for experimental conditions. Literature [31] did not include the diluted gas, while high argon fraction is used in this study. In addition, the pressures in literature [31] are slightly higher than those in this study.

Effects of pressure on ignition delays and activation energies for the 40% H_2 /60% CH_4 fuel blend are given in Fig. 6. In general, ignition delay decreases with the increase of pressure. It is observed that the promoted effect of pressure on ignition becomes significantly at high temperature conditions ($T > 1322\text{ K}$). For example, the ignition delay decreases by 33% when pressure is increased from 0.5 MPa to 2.0 MPa at 1670 K. The acceleration in chain branching reaction at high temperature is responsible for this. However, no obvious effect on ignition promotion is presented at low temperature conditions ($T < 1322\text{ K}$). For example, at temperature below 1200 K, the approximate ignition delays are presented at pressures of 1.0 MPa and 2.0 MPa, and the results are consistent with that in literature [29]. As shown in Fig. 6, EaH is increased with the increase of pressure. Similar to the 80% H_2 /20% CH_4 fuel blend, a transition in activation energy is also presented at 1277 K and 1335 K in two pressure cases (1.0 MPa and 2.0 MPa). EaH gives the value of 37.6 kcal/mol and EaL gives the value of 27.2 kcal/mol at the pressure of 1.0 MPa, while EaH takes the value of 45.7 kcal/mol and EaL takes the value of 31.9 kcal/mol at the pressure of 2.0 MPa. The results are consistent with those from Petersen et al. [31]. Their study showed that, at the pressure of 2.0 MPa, the activation energy of the 40% H_2 /60% CH_4 fuel blend was 45.1 kcal/mol at the temperatures between 1316 K and 1228 K, and gave the value of 31.1 kcal/mol at the temperatures between 1132 K and 1228 K.

The pressure dependence of the 40% CH_4 /60% H_2 fuel blend is shown in Fig. 7. The ignition delays approach to the same value regardless of pressure. In other words, the effect of pressure on ignition is little. The pressure dependence is different to those of fuel blend with hydrogen fraction less than 60%. An Arrhenius-type expression with $R^2 = 0.97$ is correlated using the multiple linear regression method based on the normalized pressure of 1.0 MPa,

$$\tau = 8.02 \times 10^{-5} p^{-0.00629} \exp\left(\frac{37.79(\text{kcal/mol})}{RT}\right) \quad (2)$$

The pressure exponent closing to zero means that the effect of pressure on ignition of the 40% CH_4 /60% H_2 fuel blend is negligible. It is well known that the pressure exponent usually takes the negative value which means the pressure can promote the ignition for the hydrocarbon dominated combustion. In contrast to this, pressure exponent gives the positive value and this indicates that

pressure can inhibit the ignition for the hydrogen dominated combustion. Due to an opposite effects of pressure on ignition for hydrogen and hydrocarbon, a negligible pressure dependence for the 40%CH₄/60H₂ fuel blend is demonstrated. Activation energy of 37.8 kcal/mol is given for the 40%CH₄/60H₂ fuel blend.

Figure 8 shows a complicated pressure dependence of the ignition delays for the 20%CH₄/80%H₂ fuel blend. Similar to the 80%CH₄/20%H₂ and 60%CH₄/40%H₂ fuel blends, a transition in activation energy for the 20%CH₄/80%H₂ fuel blend is observed when pressure is below 1.0 MPa. When hydrogen fraction is over 60%, HO₂ radical will become much important in the ignition chemistry, especially at low temperature. The chain termination reaction $H + O_2 (+M) \rightleftharpoons HO_2 (+M)$ dominates in the competition with chain branching reaction $H + O_2 \rightleftharpoons OH + O$. The former inhibits the ignition and the latter promotes the ignition. When the inhibited reaction is dominator, the total reaction rate is decreased, leading to the increase in ignition delay and the increased activation energy as shown in Fig. 8. Ignition characteristic was also studied by Skinner and Ringrose [56]. Their result shows two transitions in activation energy with the increase of temperature, and the mixtures exhibit a typical hydrogen ignition behavior at pressure of 2.0 MPa. Ignition delay decreases significantly with the increase of pressure at high temperature, and an opposite pressure dependence is presented at intermediate temperature, consequently, the ignition delays increase slightly with the increase of pressure. Study shows that the effect of pressure on the ignition of the 80%CH₄/20%H₂ fuel blend is negligible at low temperature. Fotache et al. [25] suggested that the ignition is affected through radical rather than thermal explosion for the methane–hydrogen mixtures with high hydrogen mole fraction.

Ignition delays and activation energies of hydrogen at different pressures are given in Fig. 9. The effect of pressure on the ignition of hydrogen is different at different temperatures. The effect of pressure on ignition promotion is weak at $T > 1170$ K. This behavior is different to that of 20%CH₄/80%H₂ mixture particularly at high temperature condition although hydrogen fraction is 80% in fuel blend. Since there has no carbon in hydrogen case, thus the high temperature ignition behavior of hydrocarbon fuel does not demonstrate in this study. The ignition delays of hydrogen increase with the increase of pressure at the temperatures between 1093 and 1170 K, especially at pressure of 2.0 MPa. Results also show that the ignition delay of hydrogen at pressure of 2.0 MPa is ten times longer to that at pressure of 0.5 MPa in the case of $T = 1093$ K. When $T < 1093$ K, the shortest ignition delay is exhibited at pressure of 0.5 MPa, and the longest one is exhibited at pressure of 1.0 MPa. The complex pressure dependence was also observed by Herzler and Naumann [32]. Furthermore, Meyer and Oppeheim [57] studied the ignition characteristics of the hydrogen–oxygen mixtures. Their study showed that the logarithm of ignition delay versus the reciprocal of temperature exhibited a linear relationship when pressure is below 0.05 MPa. However, a non-linear relationship was exhibited when the pressure is over 0.2 MPa. They suggested two ignition regimes, they are, the strong ignition and weak ignition regimes in the hydrogen reaction system. The pressure dependence of hydrogen is similar to that of typical hydrocarbons in the strong ignition regime.

The transition in activation energy for hydrogen is observed at $T = 1050$ K and $p = 0.5$ MPa. The value of EaH is 39.3 kcal/mol and that of EaL is 126.9 kcal/mol, while the behavior of two-steps transitions in activation energy does not demonstrated. Activation energy shows an increasing and then decreasing with increasing the temperature at pressure of 1.0 MPa. The value of EaH is 49.2 kcal/mol, the activation energy (EaM) at intermediate temperature is 258 kcal/mol and EaL is 74.5 kcal/mol. Transition temperatures are 1108 K and 1122 K. Two transitions in activation energy are also presented at pressure of 2.0 MPa. The value of EaH is

55.1 kcal/mol, EaM is 93.4 kcal/mol and EaL is 34.1 kcal/mol. Transition temperatures are 1093 K and 1170 K. Kreutz et al. [58] suggested that, when hydrogen kinetic dominates the ignition chemistry of methane–hydrogen mixtures, activation energy changing from EaL to EaM is from radicals pool enriching, while activation energy changing from EaM to EaH is from kinetic thermal feedback influencing.

As discussed above, the typical hydrocarbon ignition behavior is presented at hydrogen mole fraction less than 40% in fuel blend. Here, the methane chemistry dominates the ignition. While the typical hydrogen ignition behavior is presented at hydrogen fraction larger than 80% in fuel blend, and in this case the hydrogen chemistry dominates the ignition of the mixtures. Transition occurs from the methane dominated system to the hydrogen dominated system at hydrogen fraction of 60% in fuel blend. Fotache et al. [25] showed that a significant promotion effect on ignition was exhibited in methane–hydrogen when hydrogen mole fraction is less than 6–7%. Transition was presented when hydrogen mole fraction was between 7% and 30%, and hydrogen would dominate the ignition when hydrogen mole fraction is over 30%. Their results are different to those in this study. The main reason might be due to the different experimental facility, and different reaction time scale. The characteristic times in Fotache's et al. study [25] are considerably longer than those in this study. The present results are consistent with those of Ju and Niioka [21]. The characteristic residence times for the supersonic ignition in Ju and Niioka's study [21] are consistent with the ignition delays in shock tube in this study.

3. Computational model and validation

3.1. Chemical kinetic model

As well known, the oxidation and ignition chemistries of methane are the basic of combustion mechanism of every hydrocarbon fuels. The NUI Galway model [33] is used to make the chemical kinetics analysis of the methane–hydrogen fuel blends in this study. The detailed mechanism includes 118 species and 663 elementary reactions. The hydrogen sub-mechanism is based on O'Conaire's et al. [59] work. The NUI Galway model [33] employed for the methane–ethane system is based on the Fischer's work in study of dimethyl ether [60]. The C₃ sub-mechanism is based on the work of Curran et al. [61] using the thermodynamic parameters and rate constant rules, which were described in their study of iso-octane oxidation. The CH₃O₂ chemistry RAMEC from Petersen et al. [55] is added to the current mechanism. It is well known that CH₃O₂ species and reactions are important for accurately simulating methane oxidation at high, intermediate and low temperatures. Furthermore, Petersen et al. improved some reaction rate constants. The rate constant for the reaction



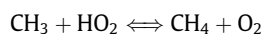
is

$$5.87 \times 10^{11} \exp(-14240 \text{ cal mol}^{-1}/RT) \text{ cm}^3 \text{ mol}^{-1} \text{ s}^{-1}.$$

The value for the reaction



is $0.9 \times 10^{13} \exp(-1200 \text{ cal mol}^{-1}/RT) \text{ cm}^3 \text{ mol}^{-1} \text{ s}^{-1}$. The rate constants for the following two reactions:



are changed so that the chain branching reaction is 2.8 times faster than the chain termination pathway.

3.2. Calculation procedure

Calculation in ignition delay, sensitivity analysis and ROP analysis of methane–hydrogen mixtures were made using CHEMKIN|| [62] program with an extensive incorporation within Senkin [63] package. For the ignition delay less than 1.5 ms, the numerical simulation of thermodynamic state for the reactive mixtures behind reflected shock wave is conducted using a zero-dimensional model with constant volume and adiabatic boundary conditions as the reaction time is much shorter than the diffusion time. Transportation including mass diffusion and heat transfer as well as viscous effect is ignored as the experimental time is in milliseconds. The constant volume, zero-dimensional chemistry model (U,V assumption) was also assumed in previous studies [29,55,64–68] and modeling data of the shock tube ignition were given by Pfahl et al. [69] and Fieweger et al. [70]. It is noted that in the inhomogeneous deflagration phase, the increase in pressure and temperature can be taken into account by the thermodynamics of process [69,70]. Noticeable deflagration phase is not observed in the present study. Furthermore, the operating conditions of shock tube are optimized according to the reactive mixtures by high concentration Ar dilution. The smooth and non-fluctuant wave pressure of reflected shock is demonstrated in Fig. 2b. Therefore, assumption of constant volume and zero-dimensional model is reasonable in calculating the ignition delay for the short ignition delay. However, for the ignition delay greater than 1.5 ms, a significant pressure rise ($dp/dt = 4\%/ms$) were observed, as shown in Fig. 2a. Here, this effect on the calculated ignition delay should be considered. The ignition delays of all mixtures of methane/hydrogen were simulated by using a modified U,V simulation (with $dp/dt = 4\%/ms$) when the ignition delays are larger than 1.5 ms.

3.3. Validation on ignition delay

Figure 10 shows the comparison between measured ignition delays and model calculation for methane using four available mechanisms (NUI Galway [33], GRI 3.0 [48], USC 2.0 [49] and Leeds 1.5 [50]). The results show that the agreement using different mechanisms is strongly dependent on hydrogen fraction and pressure. Predictions using four mechanisms show good agreement with the measured ignition delays in this study. Particularly, at the pressure less than 1.0 MPa, very good agreement is shown between the measured and the predicted. This is reasonable since these four mechanisms have been modified for methane combustion at $p \leq 1.0$ MPa.

Figure 11 shows the comparison between measured ignition delays and model calculation using four available mechanisms for hydrogen. Results show that at pressure of 0.5 MPa, the simulations using NUI Galway [33] and Leeds 1.5 [50] mechanisms agree well with the measurements. GRI 3.0 [48] mechanism over-predicts the ignition delays, and the calculated value is ten times longer than the measured ignition delay at $T = 1050$ K. USC 2.0 [49] mechanism under-predicts the ignition delays, and the calculated value is three-fifth to the measured ignition delay. At pressure of 1.0 MPa, Only the NUI Galway [33] has good prediction in ignition delays. GRI 3.0 [48] and Leeds 1.5 [50] mechanisms give a slightly high value and USC 2.0 [49] mechanism gives a slightly low value to the measured ignition delay. At pressure of 2.0 MPa, NUI Galway [33] and USC 2.0 [49] well predict the ignition delays, while mechanisms of GRI 3.0 [48] and Leeds 1.5 [50] over-predict the ignition delays at $T > 1140$ K. The four mechanisms over-predict the ignition delays at $T < 1140$ K. Recent studies [71,72] showed that the discrepancy between experiments and simulations is from the uncertain elementary reaction rate constant, and the ignition delay is limited by local ignition and different facility [71]. Therefore, further study is needed to investigate the ignition and oxidation for

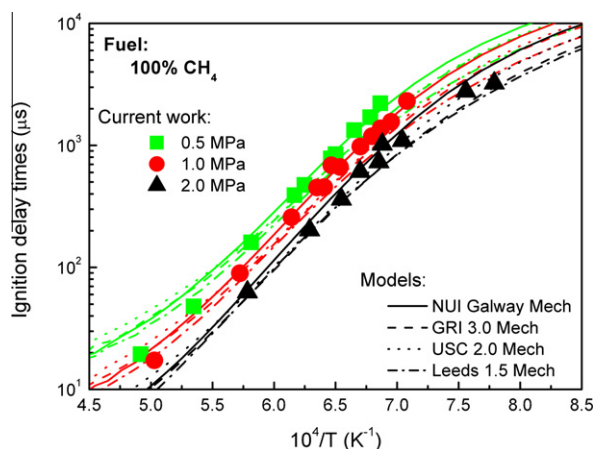


Fig. 10. Validation of ignition delays for methane.

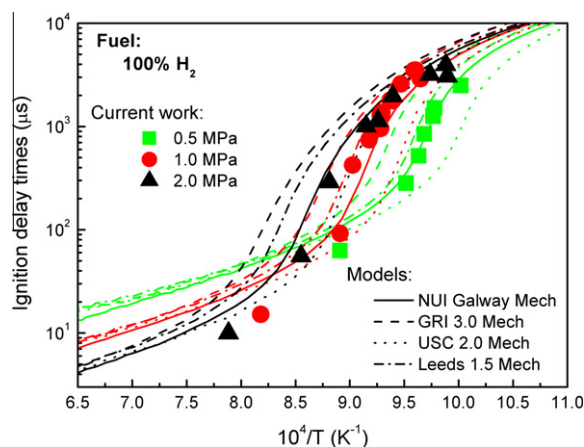


Fig. 11. Validation of ignition delays for hydrogen.

the hydrogen–oxygen fuel blend under wide conditions to validate and modify current chemical kinetic model for hydrogen oxidation.

Figure 12 gives the comparison between the measured ignition delays and model calculation using NUI Galway [33] for the methane–hydrogen fuel blend at different hydrogen fractions. The ignition delays decrease with increasing hydrogen fraction due to high reactivity, high diffusion and low auto-ignition temperature. Results also show that the promotion effect from hydrogen decreases with increasing the pressure. This behavior is supported by Huang et al. [29]. NUI Galway [33] can well predict the ignition delays at $p \leq 1.0$ MPa. However, NUI Galway [33] will over-predict the ignition delays at $p = 2.0$ MPa when hydrogen fraction in fuel blend is less than 60%, particularly at the low temperature. This is due to the uncertain rate constant of the chain termination reaction $H + O_2 (+M) \rightleftharpoons HO_2 (+M)$. Recently, Pang et al. [73] conducted an experimental and modeling study on ignition delay of the hydrogen–oxygen–argon mixtures at low temperature. They optimized the rate constant of the elementary reaction $H + O_2 + Ar \rightleftharpoons HO_2 + Ar$ in GRI 3.0 mechanism. The high pressure limiting rate constant $k_\infty = 1.04 \times 10^{13} T^{0.2} \text{ cm}^3 \text{ mol}^{-1} \text{ s}^{-1}$, low pressure limiting rate constant $k_0 = 6.99 \times 10^{18} T^{-1.2} \text{ cm}^3 \text{ mol}^{-1} \text{ s}^{-1}$ and center broadening factor F of 0.7 were used in the mechanism. The improved model can well predict the ignition delays. However, this model was only validated by the measured ignition delays at pressure of 0.35 MPa. Hong et al. [74] modified the rate constants for the following four reactions in the hydrogen oxidation mechanism:

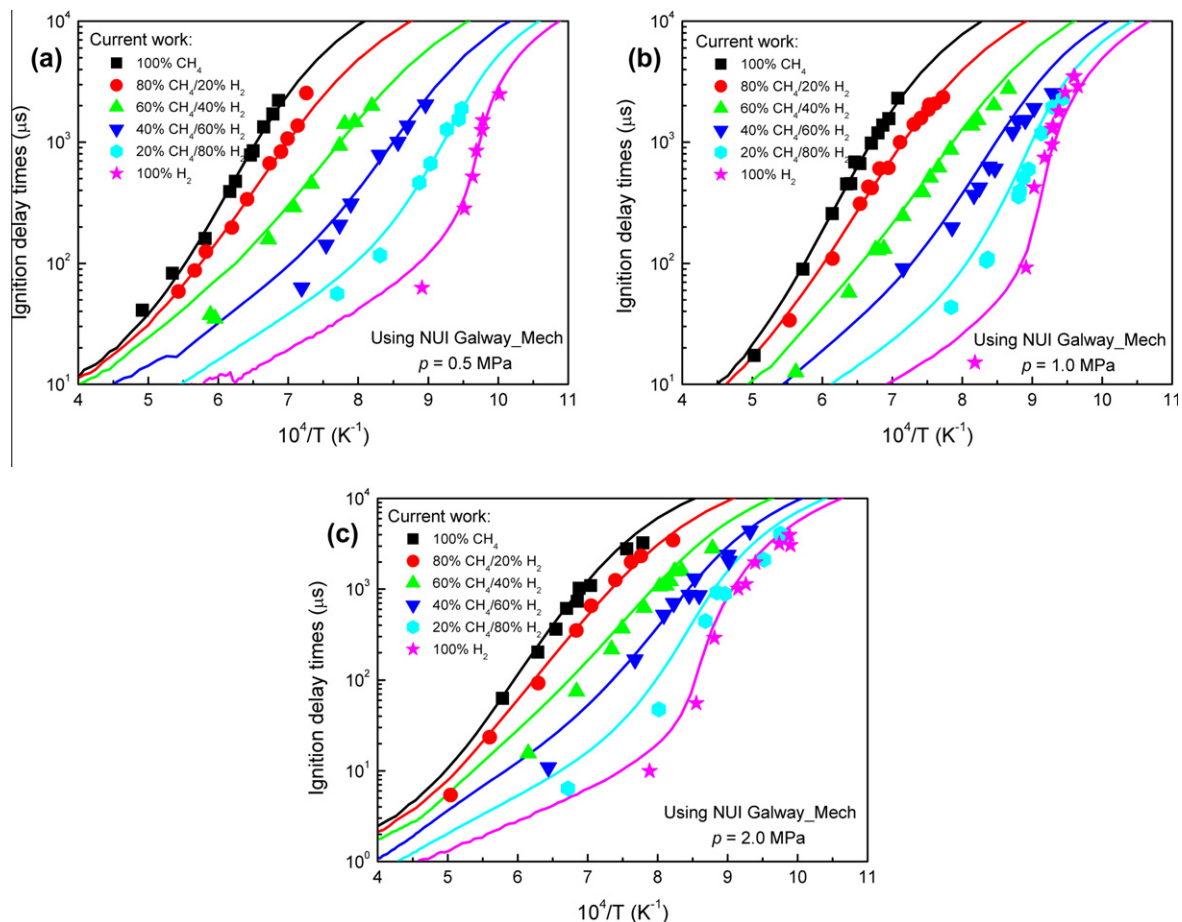
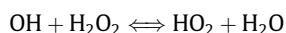
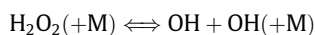


Fig. 12. Measured and simulated ignition delays for various methane–hydrogen blends at different pressures. (a) $p = 0.5$ MPa, (b) $p = 1.0$ MPa, (c) $p = 2.0$ MPa.



However, Hong et al. [74] only conducted experiments and simulations at high temperature conditions. Furthermore, the uncertain thermo-chemical parameters of some intermediate species may also result in the discrepancy of modeling calculation.

3.4. Validation of pressure

To validate the suitability of the assumption on the modified constant volume condition for the ignition delay less than 1.5 ms, the present study refers to the method of Davidson and Hanson [45], a comparison on pressure jump and plateau pressures during and after ignition is made between calculation using NUI Galway model [33] and current experimental data for six mixtures as shown in Fig. 13. The first plateau is the pressure behind the incident shock P_2 ; the second plateau is the pressure behind the reflected shock P_5 . The pressure traces are measured by pressure transducer located at position 2 from the end wall of shock tube. The plateau pressures for all mixtures show good agreement between experiments and calculations, and the timing of measured pressure jump and modeling one also exhibits good agreement except pure hydrogen with longer ignition delay (>1.5 ms). This means that NUI Galway model [33] with constant volume assumption method can well reproduce the ignition delays of the meth-

ane/hydrogen mixtures for the ignition delay less than 1.5 ms. However, for the ignition delay greater than 1.5 ms, as shown in Fig. 13f, the calculated ignition delay with using U,V assumption is longer than the measured ignition delay due to the effect of pressure rise. Therefore, the BL effect (i.e. dp/dt) needs to be considered in the calculation of long ignition delay. Furthermore, the discrepancy of the maximum value of pressure jump between measurements and simulations is also observed, particularly for the mixtures with hydrogen fraction larger than 80%. The ignition pressure jump is determined by the energy release rate of the ignition process. In the case of ignition with large energy release such as the 20%CH₄/80%H₂ fuel blend and hydrogen, the shock tube condition can not be characterized by a constant volume reactor.

Gersen et al. [75] conducted the experimental and numerical study on ignition properties of methane–hydrogen mixtures. They suggested that the NUI Galway model [33] could well predict the ignition delay for both pure hydrogen and pure methane, and thus this mechanism can give good agreement with the experimental results for the hydrogen–methane mixtures. In addition, the NUI Galway model [33] was also validated by the concentration profiles of the reactants, stable intermediates and the final products by Dagaut and Dayma [20]. Based on these work, this study also uses NUI Galway model [33] in the following chemical kinetic analysis.

4. Chemical kinetic analysis

The sensitivity analysis, the production rates and consumption rates of main intermediate species (ROP) and the concentrations

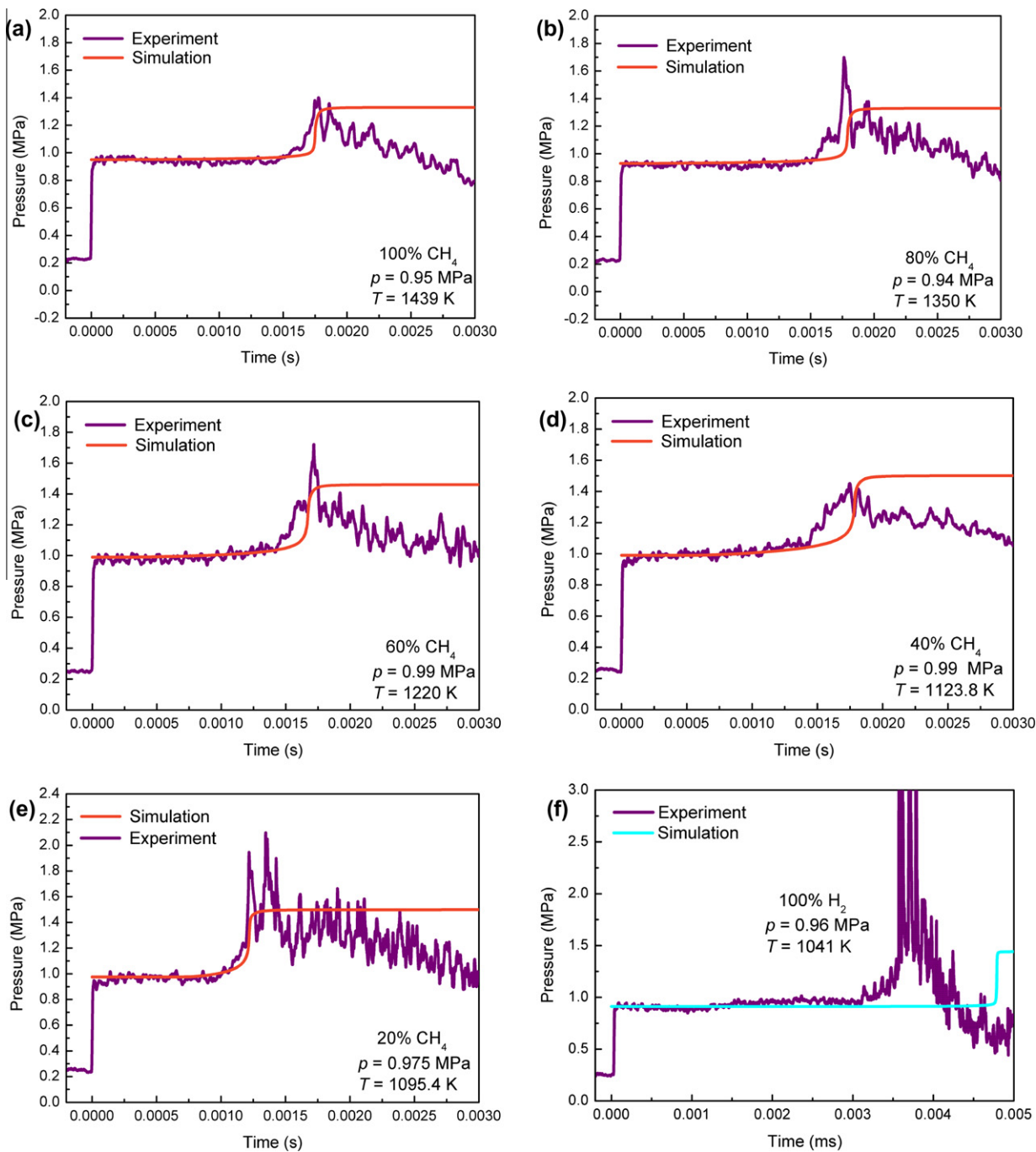


Fig. 13. Measured pressures and model prediction during ignition events of methane and hydrogen blends at 1.0 MPa. Modeling is NUI Galway model [33]. (a) Pressure comparison for 100%CH₄, (b) pressure comparison for 80%CH₄/20%H₂, (c) pressure comparison for 60%CH₄/40%H₂, (d) pressure comparison for 40%CH₄/60%H₂, (e) pressure comparison for 20%CH₄/80%H₂, (f) pressure comparison for 100%H₂.

of free radicals are the important information for understanding the mechanism of fuel ignition and oxidation.

4.1. Sensitivity analysis

Sensitivity analysis of two typical methane–hydrogen fuel blends, the 80CH₄/20H₂ fuel blend (methane dominated reaction system) and the 20CH₄/80H₂ fuel blend (hydrogen dominated reaction system) were made to examine the effect of main elementary reactions on different ignition regimes at 2.0 MPa. The normalized sensitivity is defined as,

$$S = \frac{\tau(2k_i) - \tau(0.5k_i)}{1.5\tau(k_i)} \quad (3)$$

where τ is ignition delay of the mixtures and k_i is specific rate coefficients. Negative value of sensitivity coefficient indicates a promotion effect on total reaction rate and positive value of sensitivity coefficient indicates an inhibition effect on total reaction rate.

For the methane-dominated reaction system, two most sensitive promotion reactions are recognized, as shown in Fig. 14a.



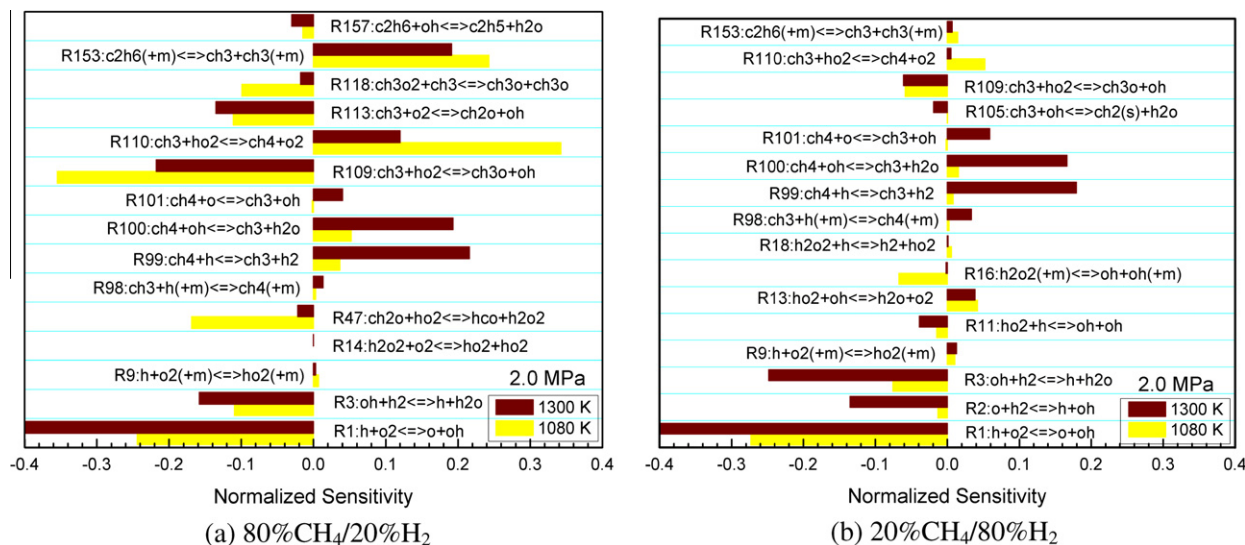
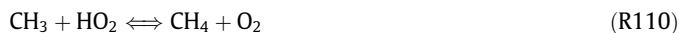


Fig. 14. Normalized sensitivity of ignition delay for two methane–hydrogen blends at two temperatures and pressure of 2.0 MPa.



As well known, the reaction (R1) is the most important chain branching reaction in combustion process for almost all hydrocarbon fuels. When a CH₃ radical, which is the controlled radical for methane oxidation, is consumed, an OH radical, which is the dominant chain branching radical, will be produced by Reaction (R109). The recombination of two CH₃ radicals through the following reactions is the important chain termination reactions in methane oxidation at high temperature conditions, thus inhibiting the ignition process.



Sensitivity coefficient of Reaction (R1) increases with increasing the temperature, leading to the acceleration of chain branching efficiency and promotion of the total reaction rate. Reactions (R109) and (R110) are a pair of reactions competing for HO₂ radical. The approximate sensitivity coefficients of the two reactions lead to a comparable contribution to the total reaction rate at $T = 1080$ K. However, sensitivity coefficients of both reactions are decreased, which leads to decreased contribution to total reaction rate at $T = 1300$ K. However, the sensitivity coefficient of the Reaction (R110) decreases more significantly and Reaction (R109) will dominate in the competition for HO₂ radical, and a whole promotion effect on the total reaction rate is presented. Sensitivity coefficient of Reaction (R153) decreases with increasing temperature, thus the inhibition effect is weakened. For the methane dominated reaction system, total reaction rate is enhanced and ignition delay is decreased with increasing temperature at the present conditions. Results of the sensitivity analysis for the 80%CH₄/20%H₂ mixture show good agreement with the experimental data as shown in Fig. 5. Furthermore, Results of the sensitivity analysis also show that sensitivity coefficients of Reactions (R99), (R100), (R101), which are main consumption reactions of methane oxidation, and they increase significantly with increasing temperature, thus the inhibition effect on total reaction rate is enhanced and activation energy of ignition is increased with increasing temperature. The accelerated ignition behavior proposed by Petersen et al. [55] is observed in this study, as shown in Figs. 4–6.

For the hydrogen dominant reactive system, as shown in Fig. 14b, Reaction (R1) has the highest sensitive coefficient, which

means that (R1) dominates absolutely in the ignition process of the mixtures. The sensitivity coefficient increases with the increase of temperature, and thus promotes the chain branching efficiency and reduces the ignition delay. The results show a good agreement with the experiments, as shown in Fig. 8. The chain termination reaction,



inhibits the total reaction rate because OH radical and HO₂ radicals are consumed by (R13). As well known, the OH and HO₂ radicals are key radicals in hydrogen oxidation and hydrogen dominated system. HO₂ radical is also consumed by inhibited (R110). The chain branching reaction,



becomes important as O radical is consumed and the more active radicals, H and OH, are formed. This leads to advance chain branching efficiency and promotes ignition. Sensitivity coefficient of the reaction,



increases with increasing temperature. Total reaction rate is increased as more active radical, H, is produced by (R3). It is noted that sensitivity coefficient of the reaction,



increases significantly with decreasing temperature. H₂O₂ is decomposed into two OH radicals by (R16), which promotes the reaction (R3) towards right direction, increases the concentration of H radical and promotes the reaction (R1). Results show a promotion effect on the ignition of the mixtures. Sensitivity coefficients of the reactions



also increase significantly with increasing temperature, thus the inhibition effect on total reaction rate is increased. This leads to the transition of activation energy for ignition. An accelerated ignition characteristic is also presented in the experiments as shown in Fig. 8.

Sensitivity analysis of ignition delay of fuel blends with different hydrogen fractions at $T = 1080$ K and $p = 2.0$ MPa is given in Fig. 15. As discussed above, the consumption of methane mainly relates to free radicals H, O and OH by (R99), (R100), (R101). Reactions (R100) and (R3) are a pair of competition reaction for OH radical in the methane–hydrogen reaction system. Reaction rate is inhibited by (R100) due to consumption of OH radical, and the reaction rate is promoted by (R3) due to production of more active radical H. Sensitivity coefficients of reactions (R3) and (R100) increase as hydrogen addition. The variation of (R3) is higher than

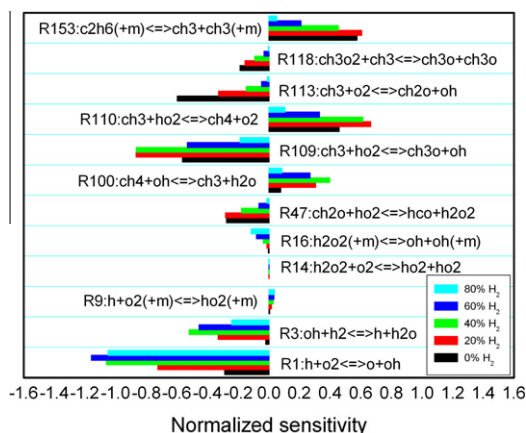


Fig. 15. Normalized sensitivity of ignition delay for methane–hydrogen blends at $T = 1080$ K and $p = 2.0$ MPa.

that of (R100), resulting in the domination of reaction (R3) to the competition for OH radical and promoting ignition. Promotion effect of reaction (R3) on total reaction rate can be explained from two aspects. One aspect is, the release heat of (R3) is higher than that of (R100) when hydrogen is added into methane. Another aspect is, active radical H produced by (R3) replaces the relative inert CH₃ radical produced by (R100) and accelerates chain branching. Sensitivity coefficient of chain termination reaction (R153) decreases as hydrogen addition. This indicates that the inhibition effect of Reaction (R153) decreases as hydrogen addition, and this is unfavorable to promotion of total reaction rate and decreasing of ignition delay. Sensitivity coefficient of Reaction (R16) increases as hydrogen addition, and this increases the concentration of OH radical and promotes chain branching. H₂O₂ radical is important in the methane–hydrogen reaction system at high pressure. Reaction (R16) will strongly influence the ignition chemistry of the mixtures. HO₂ radical is also important at low temperature and high pressure as HO₂ is a precursor radical to produce OH and H₂O₂ radicals. Sensitivity coefficient of Reaction (R110) decreases as hydrogen addition, resulting in an increased concentration of HO₂ radical, and leading to an increased concentration of OH and H₂O₂ radicals as hydrogen addition.

4.2. Ignition chemistry of methane–hydrogen fuel blends

4.2.1. Effect of hydrogen addition on concentrations of free radicals

Free radicals like H, O and OH are important for the ignition and oxidation chemistries. Almost all chain initiation, chain branching, chain propagation and chain termination reactions are initiated by

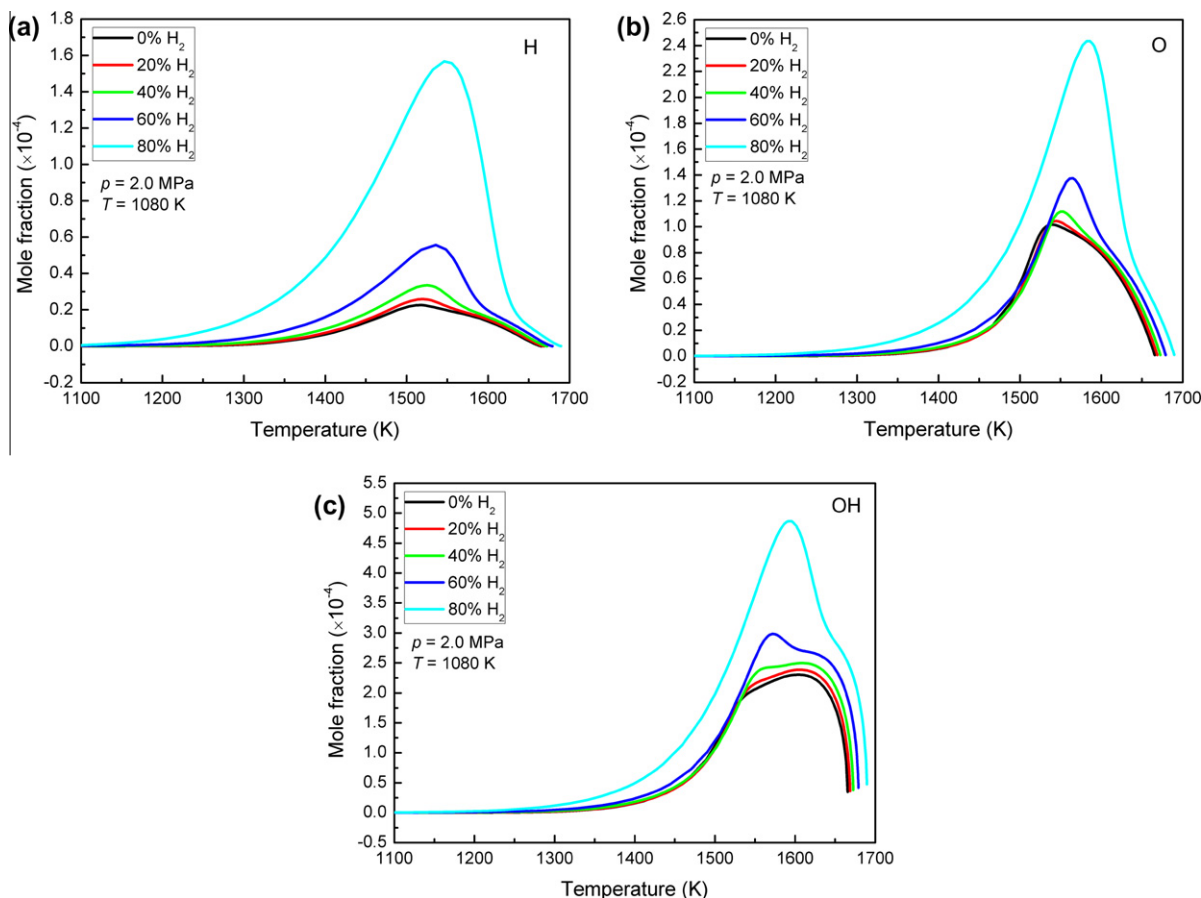


Fig. 16. Concentrations of free radicals at different hydrogen fractions. (a) Variety of the concentration of H radical, (b) Variety of the concentration of O radical, (c) Variety of the concentration of OH radical.

these free radicals. Concentrations of these free radicals play very important role in the ignition chemistry of the methane–hydrogen fuel blends.

Effects of hydrogen addition on concentrations of free radicals H, O and OH in the ignition of the methane–hydrogen fuel blends at $T = 1080\text{ K}$ and $p = 2.0\text{ MPa}$ are given in Fig. 16. Results show that concentrations of H, O and OH radicals increase with increasing hydrogen fraction. This increases total reaction rate and decreases ignition delay. Slow increase in the concentrations of these free radicals is presented for the hydrogen fractions up to 40%. But a substantial increase in the free radical concentrations is presented for the hydrogen fraction larger than 40%.

Effects of hydrogen molecular on production and consumption of H radical in the ignition abduction time indicate the contribution to the total reaction rate. Large numbers of active H and OH radicals are produced in the hydrogen oxidation and promote the ignition of the methane–hydrogen fuel blends. Rates of production and consumption of H, O and OH radicals are given in Fig. 17. Results show that H radical is produced mainly from the reactions,



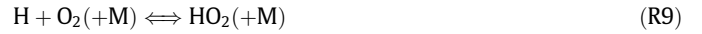
H radical is consumed by Reaction (R1). Reaction rates of (R3) and (R24) increase as hydrogen fraction is increased, producing more H radicals and promoting reaction (R1). Reaction (R24) plays the dominant role in the production of H radical when hydrogen fraction is less than 40%, and this is the key route to produce H radical. Reaction (R3) will dominate when hydrogen fraction is over 60%, and this will become the key route to produce H radical.

The key reactions for the production of O radical are,



Reaction rates of the production reaction of (R1) and the consumption reactions of (R2) and (R4) increase as hydrogen fraction is increased. Reaction rate of (R1) increases largely compared with those of (R2) and (R4), leading to the increase in the concentration of O radical and promotion in chain branching as hydrogen fraction is increased.

Study shows that (R1) is the key reaction to produce OH radical, and (R3) and (R24) are the key reactions to consume OH radical. Production rate of OH increase as hydrogen fraction is increased, leading to the increase in the concentration of OH and promoting the total reaction rate. As analyzed above, reaction rate of (R3) increases as hydrogen fraction is increased, thus forms more H and promotes Reaction (R1) to produce more O and OH radicals. This will promote methane oxidation. OH radical is mainly produced from the reactions,



as the chemistries of HO_2 and H_2O_2 radicals are important for relatively low temperature at high pressure. Here, the active H reacts

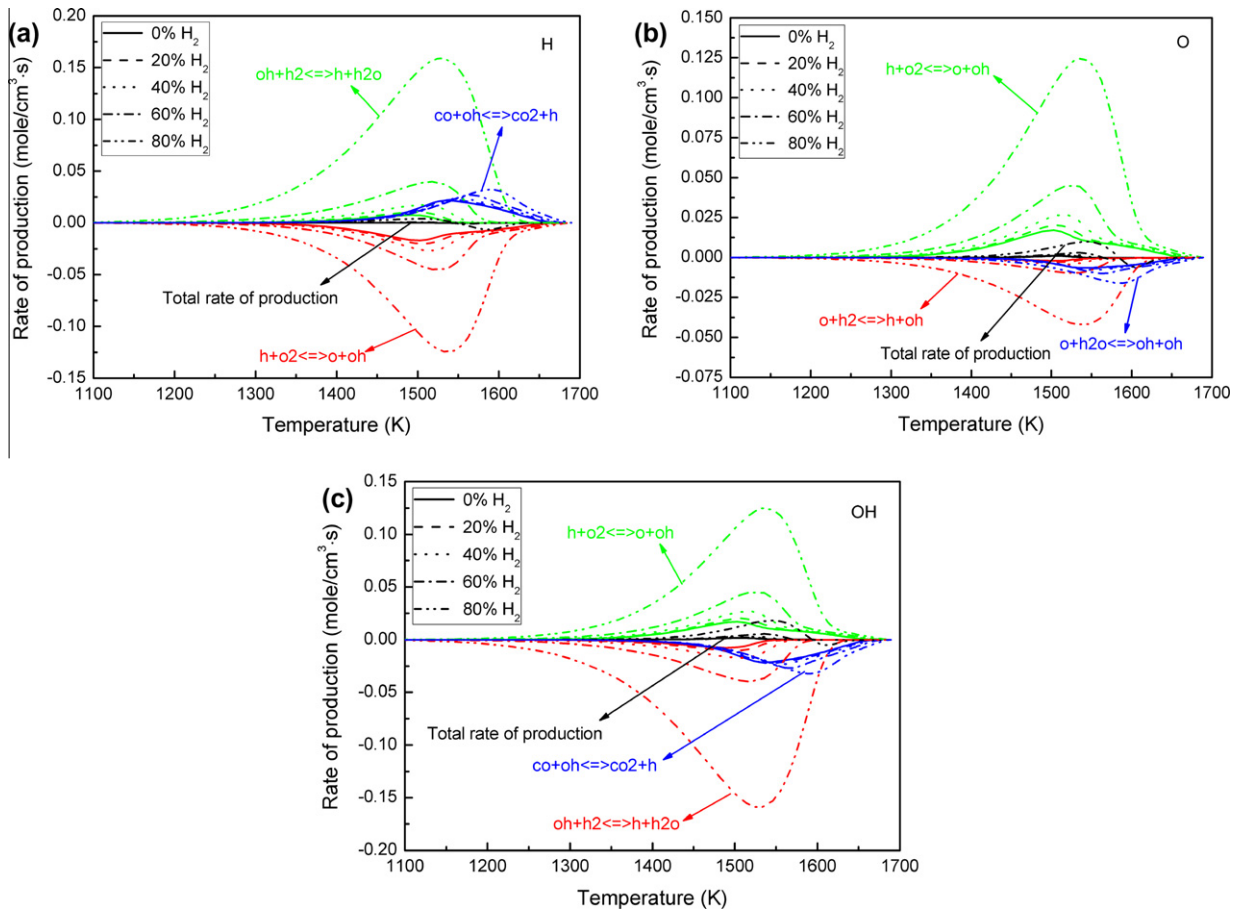


Fig. 17. Rates of production and consumption for free radicals at various hydrogen fractions and $p = 2.0\text{ MPa}$. (a) Rates of production and consumption of H radical, (b) rates of production and consumption of O radical, (c) rates of production and consumption of OH radical.

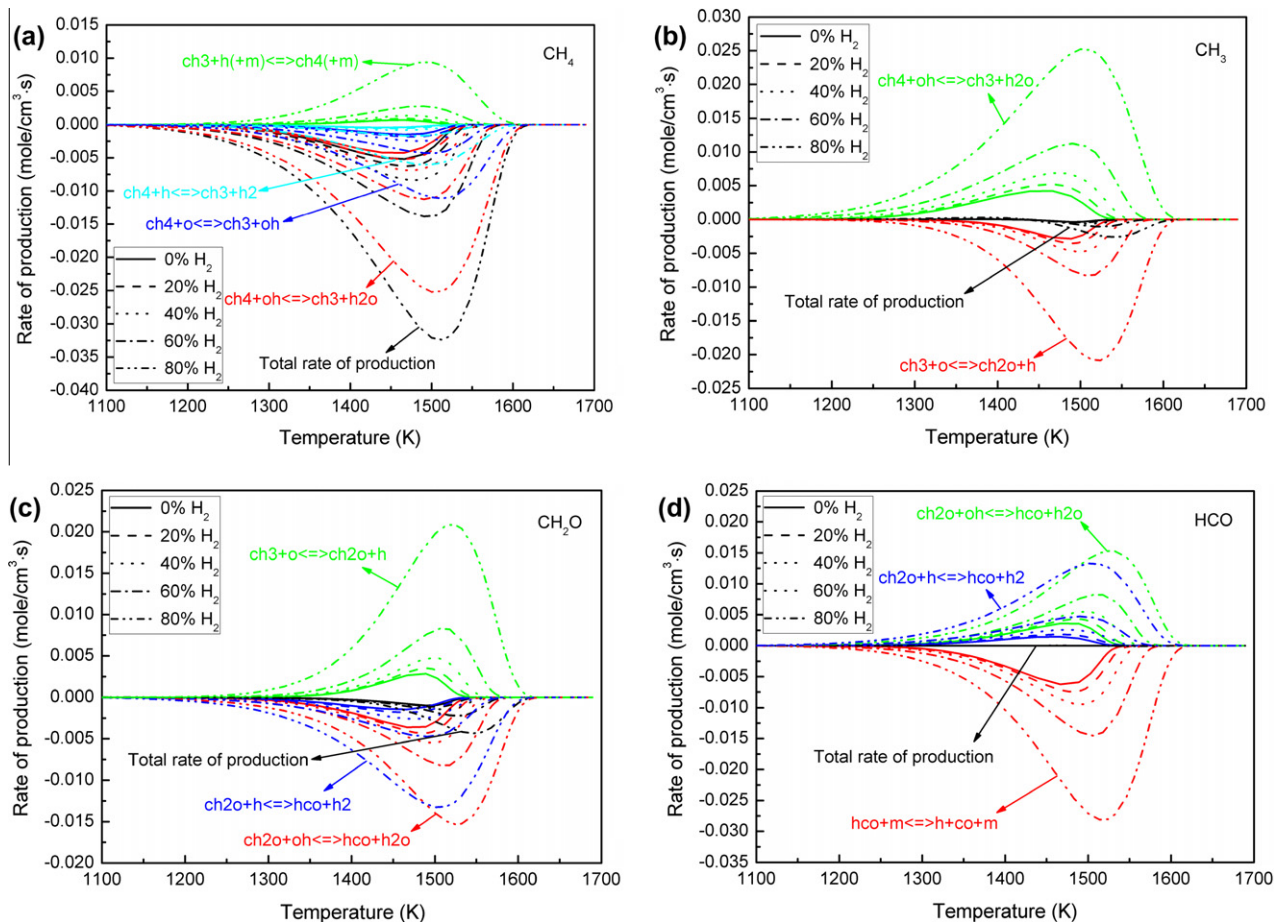


Fig. 18. Hydrogen addition on oxidation of methane at $p = 2.0$ MPa. (a) Rate of production and consumption for methane, (b) rate of production and consumption for CH₃, (c) rate of production and consumption for CH₂O, (d) rate of production and consumption for HCO.

with oxygen by (R9) rather than by (R1). Then, two HO₂ react to produce the H₂O₂ by (R14). H₂O₂ is decomposed into two OH by (R16). Meanwhile, HO₂ also reacts with H to produce two OH radicals by (R11).

4.2.2. Effect of hydrogen addition on methane oxidation

To clarify the effect of hydrogen addition on methane oxidation, the rates of production and consumption of the main C₁ species like CH₄, CH₃, CH₂O and HCO are calculated at $p = 2.0$ MPa and are plotted in Fig. 18. As discussed above, the consumption of methane in the mixtures is mainly by H, OH and O radicals in (R99), (R100), (R101). These reaction rates increase with the increase of hydrogen fraction, promoting the methane oxidation, especially for (R100). CH₃ is mainly consumed by the reaction,



Reaction (R111) is promoted as hydrogen addition. CH₂O reacts with H and OH radicals by reactions,



to product HCO radical. While Reactions (R43) and (R44) are promoted as hydrogen addition. Subsequently, HCO is decomposed into the stable CO and active H by reaction,



Results show that the enhanced oxidation of methane by hydrogen addition is realized by increasing OH radical production. This

viewpoint is supported by Dugaut et al. [19,20] and Huang et al. [29].

5. Conclusions

Experimental and kinetic study on ignition delays of lean methane–hydrogen–oxygen–argon mixtures with hydrogen mole fractions of 0%, 20%, 40%, 60%, 80% and 100% were conducted behind the reflected shock waves at temperatures from 1000 to 2000 K and pressures from 0.5 to 2.0 MPa. Main conclusions are summarized as follows.

- (1) Typical hydrocarbon ignition behavior is exhibited and ignition delays decrease with increasing pressure when hydrogen fraction is less than 40%. Transition in global activation energy is presented for 80%CH₄/20%H₂ and 60%CH₄/40%H₂ fuel blends in contrast to pure methane at 1.0 and 2.0 MPa in this study.
- (2) No influence from pressure on ignition delays is presented for the 40%CH₄/60%H₂ fuel blend. Neither hydrocarbon ignition behavior nor hydrogen ignition behavior is presented for methane–hydrogen fuel blends with hydrogen fraction of 60%.
- (3) Typical hydrogen ignition behavior and complex pressure dependence are exhibited when hydrogen fraction is over 80%. Two transitions in global activation energy are presented for the hydrogen dominated system at relatively high pressure.

- (4) Sensitivity coefficient of chain branching reaction $\text{H} + \text{O}_2 \rightleftharpoons \text{O} + \text{OH}$ increases and those of chain termination reaction $\text{C}_2\text{H}_6 (+\text{M}) \rightleftharpoons \text{CH}_3 + \text{CH}_3 (+\text{M})$ decreases with increasing temperature for the methane dominated system. This promotes the total reaction rate and decreases the ignition delays. Transition in activation energy is resulted from the interaction between promotion effect of the reactions $\text{H} + \text{O}_2 \rightleftharpoons \text{O} + \text{OH}$, $\text{O} + \text{H}_2 \rightleftharpoons \text{H} + \text{OH}$ and $\text{OH} + \text{H}_2 \rightleftharpoons \text{H} + \text{H}_2\text{O}$ and inhibition effect of the $\text{CH}_4 + \text{H} \rightleftharpoons \text{CH}_3 + \text{H}_2$ and $\text{CH}_4 + \text{OH} \rightleftharpoons \text{CH}_3 + \text{H}_2\text{O}$. Furthermore, the total reaction rate is increased due to the increasing concentration of active H through the reaction $\text{OH} + \text{H}_2 \rightleftharpoons \text{H} + \text{H}_2\text{O}$ as hydrogen addition. Methane is consumed mainly by free radicals H, O and OH. Hydrogen addition increases the concentrations of H, O and OH radicals and promotes methane oxidation.

References

- [1] H.M. Cho, B.Q. He, *Energy Convers. Manage.* 48 (2007) 608–618.
- [2] J.D. Naber, D.J. Siebers, S.S. Di Julio, C.K. Westbrook, *Combust. Flame* 99 (1994) 192–200.
- [3] K. Bier, G. Kappler, H. Wilhelmi, *AIAA J.* 9 (1971) 1865–1866.
- [4] R.A. Fraser, D.L. Siebers, C.F. Edwards, *SAE Trans.* 100 (1992) 33–38.
- [5] G.A. Karim, I. Wierzbka, Y. Al-Alousi, *Int. J. Hydrogen Energy* 21 (1996) 625–631.
- [6] S. Allenby, W.C. Chang, A. Megaritis, M.L. Wyszynski, *Proc. Inst. Mech. Eng. Part D, J. Automob. Eng.* 215 (2001) 405–418.
- [7] S. Shrestha, *Int. J. Hydrogen Energy* 24 (1999) 577–586.
- [8] S.O. Akansu, N. Kahraman, B. Ceper, *Int. J. Hydrogen Energy* 32 (2007) 4279–4284.
- [9] C.G. Bauer, T.W. Forest, *Int. J. Hydrogen Energy* 26 (2001) 55–70.
- [10] H. Ozcan, *Int. J. Hydrogen Energy* 35 (2010) 1443–1452.
- [11] E. Hu, Z. Huang, B. Liu, J. Zheng, X. Gu, B. Huang, *Int. J. Hydrogen Energy* 34 (2009) 528–539.
- [12] E. Hu, Z. Huang, B. Liu, J. Zheng, X. Gu, *Int. J. Hydrogen Energy* 34 (2009) 1035–1044.
- [13] F. Halter, C. Chauveau, N. Djebaïli-Chaumeix, I. Gökalp, *Proc. Combust. Inst.* 30 (2005) 201–208.
- [14] V. Di Sarli, A.D. Benedetto, *Int. J. Hydrogen Energy* 32 (2007) 637–646.
- [15] A.A. Konnov, R. Riemeijer, L. de Goey, *Fuel* 89 (2010) 1392–1396.
- [16] G. Yu, C.K. Law, C.K. Wu, *Combust. Flame* 63 (1986) 339–347.
- [17] E. Hu, Z. Huang, J. He, H. Miao, *Int. J. Hydrogen Energy* 34 (2009) 6951–6960.
- [18] E. Hu, Z. Huang, J. He, C. Jin, J. Zheng, *Int. J. Hydrogen Energy* 34 (2009) 4876–4888.
- [19] P. Dagaut, A. Nicolle, *Proc. Combust. Inst.* 30 (2005) 2631–2638.
- [20] P. Dagaut, G. Dayma, *Int. J. Hydrogen Energy* 31 (2006) 505–515.
- [21] Y. Ju, T. Niioka, *Combust. Flame* 102 (1995) 462–470.
- [22] J.T. Gauducheau, B. Denet, G. Searby, *Combust. Sci. Technol.* 137 (1998) 81–99.
- [23] Z. Chen, *Int. J. Hydrogen Energy* 34 (2009) 6558–6567.
- [24] J. Wang, Z. Huang, C. Tang, H. Miao, X. Wang, *Int. J. Hydrogen Energy* 34 (2009) 1084–1096.
- [25] C.G. Fotache, T.G. Kreutz, C.K. Law, *Combust. Flame* 110 (1997) 429–440.
- [26] S. Gersen, N.B. Anikin, A.V. Mokhov, H.B. Levinsky, *Int. J. Hydrogen Energy* 33 (2008) 1957–1964.
- [27] A. Lifshitz, K. Schellera, A. Burcat, G.B. Skinner, *Combust. Flame* 16 (1971) 311–321.
- [28] R.K. Cheng, A.K. Oppenheim, *Combust. Flame* 58 (1984) 125–139.
- [29] J. Huang, W.K. Bushe, P.G. Hill, S.R. Munshi, *Int. J. Chem. Kinet.* 38 (4) (2006) 221–233.
- [30] N. Chaumeix, S. Pichon, F. Lafosse, C.E. Paillard, *Int. J. Hydrogen Energy* 32 (2007) 2216–2226.
- [31] E.L. Petersen, J.M. Hall, S.D. Smith, J. de Vries, A.R. Amadio, M.W. Crofton, *J. Eng. Gas Turbines Power* 129 (2007) 937–944.
- [32] J. Herzler, C. Naumann, *Proc. Combust. Inst.* 32 (2009) 213–220.
- [33] E.L. Petersen, D.M. Kalitan, S. Simmons, G. Bourque, H.J. Curran, J.M. Simmie, *Proc. Combust. Inst.* 31 (2007) 447–454.
- [34] A Chemical Equilibrium Program for Windows. <<http://www.c.morley.dsl.pipex.com/>>.
- [35] J.P. Holman, *Experimental Methods for Engineers*, McGraw-Hill, New York, 1994.
- [36] E.L. Petersen, R.K. Hanson, *Shock Waves* 10 (2001) 405–420.
- [37] E.L. Petersen, M.J.A. Rickard, M.W. Crofton, E.D. Abbey, M.J. Traum, D.M. Kalitan, *Meas. Sci. Technol.* 16 (2005) 1716–1729.
- [38] M. Rickard, J.M. Hall, E.L. Petersen, *Proc. Combust. Inst.* 30 (2005) 1915–1923.
- [39] Gabi Ben-Dor, Ozer Igra, Tov Elperin, *Handbook of Shock Waves*. Academic Press, San Diego, 2001.
- [40] J. de Vries, E.L. Petersen, *Proc. Combust. Inst.* 31 (2007) 3163–3171.
- [41] J. de Vries, J.M. Hall, S.L. Simmons, M.J.A. Rickard, D.M. Kalitan, E.L. Petersen, *Combust. Flame* 150 (2007) 137–150.
- [42] D.C. Horning, D.F. Davidson, R.K. Hanson, *J. Propul. Power* 18 (2002) 363–371.
- [43] M. Frenklach, D.E. Bornside, *Combust. Flame* 56 (1984) 1–27.
- [44] E.L. Petersen, D.F. Davidson, R.K. Hanson, *J. Propul. Power* 15 (1999) 82–91.
- [45] D.F. Davidson, R.K. Hanson, *Int. J. Chem. Kinet.* 36 (2004) 510–523.
- [46] N. Lamoureux, C.E. Paillard, V. Vaslier, *Shock Waves* 11 (2002) 309–322.
- [47] N. Lamoureux, C.E. Paillard, *Shock Waves* 13 (2003) 57–68.
- [48] GRI-Mech 3.0. <http://www.me.berkeley.edu/gri_mech/version30/text30.html>.
- [49] Hai Wang, Xiaoqing You, Ameeya V. Joshi, Scott G. Davis, Alexander Laskin, Fokion Egolfopoulos, Chung K. Law, *USC Mech Version II. High-temperature Combustion Reaction Model of H₂/CO/C1–C4 Compounds*, May 2007. <http://ignis.usc.edu/USC_Mech_II.htm>.
- [50] K.J. Hughes, T. Turányi, A.R. Clague, M.J. Pilling, *Int. J. Chem. Kinet.* 33 (2001) 513–538.
- [51] A. Grillo, M.W. Slack, *Combust. Flame* 27 (1976) 377–381.
- [52] D.J. Seery, C.T. Bowman, *Combust. Flame* 14 (1970) 37–47.
- [53] E.L. Petersen, M. Rohrig, D.F. Davidson, R.K. Hanson, C.T. Bowman, *Symp. Int. Combust.* 26 (1996) 799–806.
- [54] J. Huang, P.G. Hill, W.K. Bushe, S.R. Munshi, *Combust. Flame* 136 (2004) 25–42.
- [55] E.L. Petersen, D.F. Davidson, R.K. Hanson, *Combust. Flame* 117 (1999) 272–290.
- [56] G.B. Skinner, G.H. Ringrose, *J. Chem. Phys.* 42 (1965) 2190–2192.
- [57] J.W. Meyer, A.K. Oppenheim, *Symp. Int. Combust.* 13 (1971) 1153–1164.
- [58] T.G. Kreutz, M. Nishioka, C.K. Law, *Combust. Flame* 99 (1994) 758–766.
- [59] M.O. Conaire, H.J. Curran, J.M. Simmie, W.J. Pitz, C.K. Westbrook, *Int. J. Chem. Kinet.* 36 (2004) 603–622.
- [60] S.L. Fischer, F.L. Dryer, H.J. Curran, *Int. J. Chem. Kinet.* 32 (2000) 713–740.
- [61] H.J. Curran, P. Gaffuri, W.J. Pitz, C.K. Westbrook, *Combust. Flame* 129 (2002) 253–280.
- [62] R.J. Kee, F.M. Rupley, J.A. Miller, *CHEMKIN II. Sandia National Laboratory Report SAND 89-8009*, 1989.
- [63] A.E. Lutz, R.J. Kee, J.A. Miller, *Senkin: A Fortran Program for Predicting Homogeneous Gas Phase Chemical Kinetics with Sensitivity Analysis*, Sandia National Laboratories Report SAND87-8248, 1987.
- [64] H.K. Ciezki, G. Adomeit, *Combust. Flame* 93 (1993) 421–433.
- [65] K. Fieweger, R. Blumenthal, G. Adomeit, *Symp. Int. Combust.* 25 (1994) 1579–1585.
- [66] C. Chevalier, W.J. Pitz, J. Warnatz, C.K. Westbrook, H. Melenk, *Symp. Int. Combust.* 24 (1992) 93–101.
- [67] H. Pitsch, *Symp. Int. Combust.* 26 (1996) 721–728.
- [68] M. Nehse, J. Warnatz, C. Chevalier, *Symp. Int. Combust.* 26 (1996) 773–780.
- [69] U. Pfahl, K. Fieweger, G. Adomeit, *Symp. Int. Combust.* 26 (1996) 781–789.
- [70] K.R. Fieweger, G. Adomeit, *Combust. Flame* 109 (1997) 599–619.
- [71] F.L. Dryer, M. Chaos, *Combust. Flame* 152 (2008) 293–299.
- [72] K. Gkagkas, R.P. Lindstedt, *Combust. Theory Model* 13 (2009) 607–643.
- [73] G.A. Pang, D.F. Davidson, R.K. Hanson, *Proc. Combust. Inst.* 32 (2009) 181–188.
- [74] Z. Hong, D.F. Davidson, R.K. Hanson, *Combust. Flame* 158 (2011) 633–644.
- [75] S. Gersen, *Experimental Study of the Combustion Properties of Methane/Hydrogen Mixtures*, University of Groningen, Groningen, 2007.